

## Chapter 1

### Pupil Plane Phase Apodization

Matthew A. Kenworthy, Johanan L. Codona\* and Frans Snik

*Leiden Observatory, Leiden University,  
P.O. Box 9513, 2300 RA Leiden, The Netherlands,  
kenworthy@strw.leidenuniv.nl*

Phase apodization coronagraphs are implemented in a pupil plane to create a dark hole in the science camera focal plane. They are successfully created as “Apodizing Phase Plates” (APPs) using classical optical manufacturing, and as “vector-APPs” using liquid-crystal patterning with essentially achromatic performance. This type of coronagraph currently delivers excellent broadband contrast ( $\sim 10^{-5}$ ) at small angular separations (few  $\lambda/D$ ) at ground-based telescopes, owing to their insensitivity to tip/tilt errors.

#### 1. Introduction

Pupil-plane apodization techniques (amplitude, phase, or complex) differ from focal plane mask coronagraphs in that they affect all objects in the field in an identical fashion. The main goal of such pupil-plane coronagraphs is to enforce dark holes in the ensuing point spread function (PSF) in which faint companions can be directly detected and characterized. Since the star and companion have the same PSF, the halo should be suppressed while preserving the starlight in the core as much as possible, *i.e.* a high Strehl ratio PSF. In this situation, the “noise” is governed by the PSF diffraction halo plus any diffuse background, while the “signal” is contained in the PSF core.

The phase-only “Apodizing Phase Plate”<sup>1–4</sup> (APP) coronagraphs have now been successfully applied on-sky at ground-based telescopes. The main benefits of APPs include a high contrast inside the dark hole ( $\sim 10^{-4}$ – $10^{-6}$ ), at a small inner working angle  $\sim 1.5\lambda/D$ , with complete insensitivity to tip/tilt errors (and partially resolved stellar disks) that usually limit focal-plane coronagraphs. This invariance of the PSF additionally enables beam-switching for thermal background removal, and observations of multiple star systems. With the introduction of advanced liquid-crystal technology for the vector-APP coronagraph,<sup>5–7</sup> it has also become efficient over spectral bandwidths of more than an octave, at wavelengths from 300 to 30,000 nm.<sup>8</sup> The extreme phase patterns enabled by liquid-crystal writing techniques can

\*Steward Observatory, 933 N. Cherry Avenue, Tucson, AZ 85721, USA

now also produce dark holes with various shapes, including complementary  $180^\circ$  D-shaped dark holes and  $360^\circ$  donut-shaped dark holes. As a single pupil-plane optic, the (vector-)APP is easily implemented in a filter wheel in existing instruments, and is fully compatible with cryovacuum (and likely also space-based) operation.

## 2. Theory

The 1-D apodization problem has been studied for a long time, including slit apodization in spectroscopy and pulse shaping to reduce channel bandwidth in telegraphy, by apodizing in amplitude.<sup>9</sup> The family of functions to describe this are the Slepian functions and the Prolate Spheroidal wavefunction.<sup>10</sup> Since transmission apodization is linear, it can achieve a high degree of suppression between the PSF and the halo beyond a selected inner working angle (IWA), and in general the apodizations are complex with both transmission and phase. The accurate manufacture of complex amplitude masks is non-trivial and can result in low transmission efficiencies.

Phase-only apodization theory was initially developed for removing speckles generated by residual optical aberrations in high contrast imaging experiments,<sup>11</sup> where wavefront sensing in the final focal plane of a coronagraph forms a closed loop with a deformable mirror (DM) in the optical system. A sinusoidal ripple on the DM forms a diffraction grating in the phase of the wavefront, generating a pair of speckles that are copies of the Airy core of the central PSF. The appropriate choice of spatial phase and amplitude of the ripple applied to the DM destructively interferes with speckles generated by aberrations in the optical system. The same principle can be generalized to cancel out the diffraction rings of the PSF itself, as demonstrated on-sky by the addition of coma into an adaptive optics system to cancel out part of the first Airy ring.<sup>12</sup> Apodization in phase over a two-dimensional region does not yet have an analytic solution. Superposing many different phase ripples in the pupil plane to suppress the diffraction pattern over a region of interest (ROI - typically defined as a D-shaped region next to the Airy core of the PSF) is challenging, since the speckles add vectorially and interfere with each other, making it a nonlinear problem. Ref. 13 searched for phase-only apodization solutions through a modal basis approach. An ROI is defined in a complex amplitude focal plane, where the diffraction halo is to be minimized. A complex amplitude field is defined in the pupil plane, and a Fourier imaging operator is defined that maps from the pupil plane into the ROI. Singular Value Decomposition of this operator produces a modal basis set of complex pupil amplitudes, ordered canonically from the most power contained within the ROI to the least. These modes typically have complex amplitudes in the pupil plane, so their complex amplitude is normalized to unity to make them phase-only apodization. These “antihalo” modes are subtracted off the complex amplitude of the pupil plane, and the process is repeated. The antihalo modes extend a short distance beyond the ROI, and if the IWA is within the first Airy ring, flux from the core of the PSF is detrimentally removed as well. Care is

needed to suppress these modes by imposing additional constraints to maximize the PSF core encircled energy. If not properly accounted for, phase wrapping can also occur when the peak-to-valley phase apodization is greater than  $2\pi$ .

New algorithms have been developed at Leiden Observatory by Doelman, Keller and Por. Doelman generates focal plane dark zones using a combination of phase-only pupil modes.<sup>14</sup> A simulated annealing approach is used, where the mode amplitudes are randomly adjusted. Solutions that improve the dark region are kept, but worse solutions are occasionally accepted as well to escape local minima. Keller uses a Gerchberg-Saxton<sup>15</sup> method, switching between the pupil plane and focal plane. Convergence to a given contrast level is increased by an order of magnitude using Douglas-Rachford operator splitting.<sup>16</sup> Por<sup>17</sup> generalizes an algorithm by Carlotti<sup>18</sup> for general complex amplitudes in the pupil plane. Strehl ratio maximisation for this mask is a linear operation solved by large scale optimizer, and phase-only solutions are naturally found through this approach.

### 3. First generation APPs using classical phase

The manufacture of APP solutions requires the variation of phase across the pupil plane of the camera, and the development of free-form optic manufacture with notable departures from sphericity using computer-controlled diamond turning<sup>19</sup> encoded the phase patterns as variations in the thickness of a high refractive index transmissive substrate. First light observations of an APP with diamond turned optics<sup>1</sup> demonstrated the viability of the manufacturing technique and of the theory. The success of the prototype led to APP coronagraphs on the 6.5m MMTO telescope in Arizona<sup>2</sup> and on the Very Large Telescope in Chile.<sup>3,4</sup> The VLT APP led to the first coronagraphic image of the extrasolar planet  $\beta$  Pictoris b<sup>20</sup> and the discovery of the extrasolar planet HD 100546b.<sup>21</sup>

Diamond turning only allows for low spatial frequencies in the azimuthal direction of the cutting tip, and the classical phase plate manufacturing was inherently chromatic. Attempts to achromatize the APP using doublets proved highly challenging.<sup>22</sup>

### 4. The Vector-APP

The main limitations of the APP coronagraph (chromaticity, limited coverage around the star, limited phase pattern accuracy) were solved by the introduction of the vector-APP (vAPP).<sup>5</sup> In a similar way as for the Vector Vortex Coronagraph,<sup>23</sup> the vAPP replaces the classical phase pattern ( $\phi_c[u, v] = n(\lambda)\Delta d[u, v]$ ) with the so-called Pancharatnam<sup>24</sup>-Berry<sup>25</sup> phase or “geometric phase”.<sup>26</sup> The vAPP phase pattern is imposed by a half-wave retarder with a patterned fast axis orientation  $\theta[u, v]$ . The geometric phase is imprinted on incident beams decomposed according to circular polarization state:  $\phi_g[u, v] = \pm 2 \cdot \theta[u, v]$ , with the sign depending on the circular polarization handedness. As this fast axis orientation pattern does not

vary as a function of wavelength (with the possible exception of an inconsequential offset/piston term), the geometric phase is strictly achromatic. A simple Fraunhofer propagation from the pupil  $[u, v]$  to the focal plane  $[x, y]$  shows that after splitting circular polarization states the two ensuing coronagraphic PSFs are point-symmetric ( $PSF_L[x, y] = PSF_R[-x, -y]$ ), and therefore, in the case of D-shaped dark holes, delivers complementary PSFs that furnish instantaneous  $360^\circ$  search space around each star.

Vector-APP devices are produced by applying two breakthrough liquid-crystal techniques: any desired phase pattern is applied onto a substrate glass through a *direct-write procedure*<sup>27</sup> that applies the orientation pattern  $\theta[u, v]$  by locally polymerizing the alignment layer material in the direction set by the controllable polarization of a scanning UV laser. Consecutively, birefringent liquid-crystal layers are deposited on top of this alignment layer. Several self-aligning layers (“*Multi-Twist Retarders*”; MTR<sup>28</sup>) with predetermined parameters (birefringence dispersion, thickness, nematic twist) yield a linear retardance that is close to half-wave over the specified wavelength range. The vAPP can become efficient over a large wavelength range (up to more than an octave), while any phase pattern can be written with high accuracy.

#### 4.1. Prototyping and first on-sky results

The first broad-band vAPP device was fully characterized in the lab at visible wavelengths (500–900 nm).<sup>6</sup> The main limitation of the contrast performance inside the dark hole was the occurrence of leakage terms that produced a faint copy of the regular PSF on top of the coronagraphic PSFs. These leakage terms are caused by small offsets to the half-wave retardance of the vAPP device, and offsets from quarter-wave retardance of the quarter-wave plate that, together with a Wollaston prism, accomplishes the (broad-band) circular polarization splitting. This issue was resolved with the introduction of the “grating-vAPP”,<sup>29</sup> which implements the circular polarization splitting by superimposing a tilt (i.e. a “polarization grating”<sup>8</sup>) pattern on top of the coronagraphic pupil phase pattern, which, by virtue of the properties of the geometric phase, very efficiently sends the coronagraphic PSFs into grating orders  $\pm 1$ , and leaves all the leakage terms in the zeroth order. The grating-vAPP also greatly simplifies the optical configuration, as all the manipulation takes place within one single (flat) optic. The coronagraphic PSFs are now subject to a lateral grating dispersion term and so the grating-vAPP can only be used in combination with narrow-band filters, although the wavelength range throughout which these filters can be applied can still be very large.

The first grating-vAPP successfully demonstrated on-sky was installed at the MagAO/Clio instrument attached to the 6.5-m Magellan-Clay telescope in Chile<sup>7</sup> (Fig. 1a–c). The device was designed and built to operate from 2–5  $\mu\text{m}$ , covering the infrared atmospheric K, L and M-bands. The first-light observations demonstrated excellent suppression of the stellar diffraction halo in the complementary

dark holes (see Fig. 1c). Detailed analysis of the data demonstrated a  $5\text{-}\sigma$  contrast for point source detection of  $\sim 10^{-5}$  at  $2.5\text{--}7 \lambda/D$ .<sup>7</sup> The contrast performance is greatly enhanced by combining the two complementary dark holes through a simple rotation-subtraction procedure to further suppress the wind-driven starlight halo in the dark holes, which is caused by finite AO loop speed. Figure 1c shows the presence of the leakage term PSF in between the coronagraphic PSFs, which can be used as an astrometric and photometric reference, in the (frequent) case that the coronagraphic PSF cores are saturated.

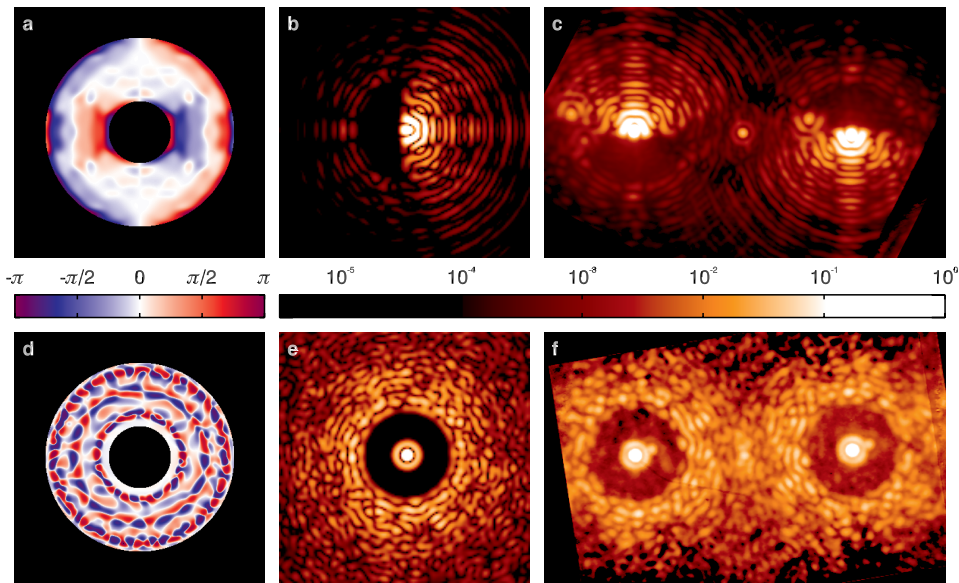


Fig. 1. Phase patterns, theoretical and on-sky PSFs (logarithmic scale) for the two vAPP devices installed at MagAO. a) Theoretical phase pattern for a  $180^\circ$  dark hole covering  $2\text{--}7 \lambda/D$ , b) the ensuing theoretical PSF, c) the on-sky PSFs at MagAO for the star  $\eta$  Crucis at  $3.9 \mu\text{m}$ . d) Theoretical phase pattern for a  $360^\circ$  dark hole covering  $3\text{--}7 \lambda/D$ , e) the ensuing theoretical PSF, f) the on-sky PSFs at MagAO for the binary star  $\beta$  Centauri at  $3.9 \mu\text{m}$ . Phase pattern designs by Christoph Keller. Data processing by Gilles Otten.<sup>7</sup>

#### 4.2. 360 degree APP solutions

As part of the algorithm exploration of the APP surface, a family of functions was found that showed  $360^\circ$  of suppression around the central star. These solutions have lower Strehl ratios for the star (typically  $20\text{--}40\%$ ) with larger IWA compared to the  $180^\circ$  dark holes, and these phase pattern solutions are pathological in nature, with rapid phase changes over small scales. The advent of liquid-crystal patterning encouraged us to revisit these  $360^\circ$  solutions, and test them in the lab and on-sky. Figure 1d-f shows the phase pattern and ensuing PSFs for the experimental

vAPP device at MagAO. The lower row of figures shows that the liquid-crystal manufacture successfully reproduces the complex phase pattern, and this on-sky image (Fig. 1f) shows a fainter binary stellar companion to the right of the primary star’s PSF.

## 5. Future Directions

Our team is currently installing different vAPP coronagraphs at several instruments at large telescopes around the world, and working on novel designs for the future extremely large telescopes. Foreseeable future developments of the vector-APP as a separate optical component, and as integral part of a high-contrast imaging system include:

- The combination of several grating layers in a “*double-grating-vAPP*” to recombine the two coronagraphic PSFs with  $360^\circ$  dark holes to feed an integral-field unit while rejecting the leakage terms.
- By prescribing a specific retardance profile as a function of wavelength, it is possible to build a *wavelength-selective vAPP* device, that operates as a regular vAPP coronagraph at the science wavelengths, and acts like a regular glass plate at the spectral range of a wavefront sensor behind it.
- The pupil phase manipulation of the vAPP can be extended by amplitude manipulation in the pupil to create complex apodizers,<sup>18</sup> and by phase/amplitude masks in the focal plane to yield *hybrid coronagraphy*.<sup>30</sup>
- As this technology is likely compatible with operation in space, it is opportune to characterize the performance of vAPP-like coronagraphs at the *extreme contrast levels* ( $\sim 10^{-9}$ ) of space-based high-contrast imaging.
- To adapt the vAPP phase pattern to the observational needs, the observing conditions, and segmented pupils with variable configurations, active liquid-crystal devices will be developed to establish “*adaptive coronagraphy*”. Such a system can then deliver dark holes of various geometry and depth, depending on whether the observer is interested in detecting exoplanets or characterizing known targets.
- As the vAPP relies on polarization splitting, it is possible to design an optimal system for *coronagraphic polarimetry*,<sup>31</sup> particularly with the  $360^\circ$ -designs.
- The fact that the vAPP produces several PSFs for the same star at the focal plane makes it an attractive option for implementing *focal-plane wavefront sensing*, for instance through phase-diversity techniques. Another promising approach involves the incorporation of an additional pupil phase pattern which generates pairs of PSF copies around the main PSFs, with each pair encoding a wavefront error mode through an intensity difference.<sup>32</sup>

## 6. Acknowledgments

The research of FS leading to these results has received funding from the European Research Council under ERC Starting Grant agreement 678194 (FALCONER).

## References

1. M. A. Kenworthy, J. L. Codona, P. M. Hinz, J. R. P. Angel, A. Heinze, and S. Sivanandam, First On-Sky High-Contrast Imaging with an Apodizing Phase Plate, *ApJ* . **660**, 762–769 (May, 2007). doi: 10.1086/513596.
2. M. A. Kenworthy, T. Meshkat, J. H. Quanz, S. P. and Girard, M. R. Meyer, and M. Kasper, Coronagraphic Observations of Fomalhaut at Solar System Scales, *ApJ* . 764:7 (Feb., 2013). doi: 10.1088/0004-637X/764/1/7.
3. M. Kenworthy, S. Quanz, M. Meyer, M. Kasper, J. Girard, R. Lenzen, J. Codona, and P. Hinz, A New Coronagraph for NAOS-CONICA – the Apodising Phase Plate, *The Messenger*. **141**, 2–4 (sep, 2010).
4. M. A. Kenworthy, S. P. Quanz, M. R. Meyer, M. E. Kasper, R. Lenzen, J. L. Codona, J. H. Girard, and P. M. Hinz. An apodizing phase plate coronagraph for VLT/NACO. In *Society of Photo-Optical Instrumentation Engineers (SPIE) Conference Series*, vol. 7735, *Presented at the Society of Photo-Optical Instrumentation Engineers (SPIE) Conference* (July, 2010). doi: 10.1117/12.856811.
5. F. Snik, G. Otten, M. Kenworthy, M. Miskiewicz, M. Escuti, C. Packham, and J. Codona. The vector-APP: a broadband apodizing phase plate that yields complementary PSFs. In *Proc. SPIE*, vol. 8450, *Proc. SPIE* (Sept., 2012). doi: 10.1117/12.926222.
6. G. P. P. L. Otten, F. Snik, M. A. Kenworthy, M. N. Miskiewicz, and M. J. Escuti, Performance characterization of a broadband vector apodizing phase plate coronagraph, *Opt. Express*. **22**(24), 30287–30314 (Dec, 2014). doi: 10.1364/OE.22.030287. URL <http://www.opticsexpress.org/abstract.cfm?URI=oe-22-24-30287>.
7. G. P. P. L. Otten, F. Snik, M. A. Kenworthy, C. U. Keller, J. R. Males, K. M. Morzinski, L. M. Close, J. L. Codona, P. M. Hinz, K. J. Hornburg, L. L. Brickson, and M. J. Escuti, On-sky Performance Analysis of the Vector Apodizing Phase Plate Coronagraph on MagAO/Clio2, *ApJ* . 834:175 (Jan., 2017). doi: 10.3847/1538-4357/834/2/175.
8. C. Packham, M. Escuti, J. Ginn, C. Oh, I. Quijano, and G. Boreman, Polarization Gratings: A Novel Polarimetric Component for Astronomical Instruments, *PASP*. **122**, 1471–1482 (Dec., 2010). doi: 10.1086/657904.
9. P. Jacquinot and B. Roizen-Dossier, *Progress in Optics*, vol. 3, chapter 2, pp. 29–186. North Holland Publishing Company, (1964).
10. D. Slepian, Analytic solution of two apodization problems, *J. Opt. Soc. Am.* **55**(9), 1110–1115, (1965).
11. F. Malbet, J. W. Yu, and M. Shao, High-Dynamic-Range Imaging Using a Deformable Mirror for Space Coronagraphy, *PASP* . **107**, 386 (Apr., 1995). doi: 10.1086/133563.
12. E. Serabyn, K. Wallace, M. Troy, B. Mennesson, P. Haguenaer, R. Gappinger, and R. Burruss, Extreme Adaptive Optics Imaging with a Clear and Well-Corrected Off-Axis Telescope Subaperture, *ApJ* . **658**, 1386–1391 (Apr., 2007). doi: 10.1086/511949.
13. J. Codona. Phase Apodization Coronagraphy. In *In the Spirit of Bernard Lyot: The Direct Detection of Planets and Circumstellar Disks in the 21st Century*, p. 24 (June, 2007).

14. D. Doelman. Optimizing apodizing phase plate designs with simulated annealing. Master's thesis, Leiden Observatory, Leiden, The Netherlands, (2016).
15. R. W. Gerchberg and W. O. Saxton, A practical algorithm for the determination of the phase from image and diffraction plane pictures, *Optik (Jena)*. **35**, 237+, (1972).
16. J. Douglas and H. Rachford, On the numerical solution of heat conduction problems in two or three space variables, *Trans. Amer. Math. Soc.* **82**(2), 421–439, (1956).
17. E. H. Por. Optimal design of apodizing phase plate coronagraphs. In *Society of Photo-Optical Instrumentation Engineers (SPIE) Conference Series*, vol. 10400, p. 104000V (Sept., 2017). doi: 10.1117/12.2274219.
18. A. Carlotti, N. J. Kasdin, R. J. Vanderbei, and A. J. Eldorado Riggs. Hybrid coronagraphic design: optimization of complex apodizers. In *Proc. SPIE*, vol. 8864, *Proc. SPIE* (Sept., 2013). doi: 10.1117/12.2024523.
19. G. E. Davis, M. A. Kenworthy, and A. R. Hedges. Manufacturing of a freeform phase plate for suppression of diffraction in an astronomical telescope. In *Proc. SPIE TD04, Optifab 2007: Technical Digest, TD041J; James J. Kumler; Matthias Pfaff, Eds.* (May, 2007).
20. S. P. Quanz, M. R. Meyer, M. A. Kenworthy, J. H. V. Girard, M. Kasper, A.-M. Lagrange, D. Apai, A. Boccaletti, M. Bonnefoy, G. Chauvin, P. M. Hinz, and R. Lenzen, First Results from Very Large Telescope NACO Apodizing Phase Plate: 4  $\mu\text{m}$  Images of The Exoplanet  $\beta$  Pictoris b, *ApJL* . **722**, L49–L53 (Oct., 2010). doi: 10.1088/2041-8205/722/1/L49.
21. S. P. Quanz, J. R. Crepp, M. Janson, H. Avenhaus, M. R. Meyer, and L. A. Hillenbrand, Searching for Young Jupiter Analogs around AP Col: L-band High-contrast Imaging of the Closest Pre-main-sequence Star, *ApJ* . 754:127 (Aug., 2012). doi: 10.1088/0004-637X/754/2/127.
22. M. A. Kenworthy, P. M. Hinz, J. L. Codona, J. C. Wilson, M. F. Skrutskie, and E. Solheid. Developing achromatic coronagraphic optics for LMIRCam and the LBT. In *Society of Photo-Optical Instrumentation Engineers (SPIE) Conference Series*, vol. 7734, *Presented at the Society of Photo-Optical Instrumentation Engineers (SPIE) Conference* (July, 2010). doi: 10.1117/12.856819.
23. D. Mawet, E. Serabyn, K. Liewer, C. Hanot, S. McEldowney, D. Semo, and N. O'Brien, Optical Vectorial Vortex Coronagraphs using Liquid Crystal Polymers: theory, manufacturing and laboratory demonstration, *Optics Express*. **17**, 1902–1918 (Feb., 2009). doi: 10.1364/OE.17.001902.
24. S. Pancharatnam, Generalized theory of interference, and its applications. part i. coherent pencils, *Proceedings of the Indian Academy of Sciences, Section A*. **44**(5), 247–262, (1956).
25. M. V. Berry, Quantal phase factors accompanying adiabatic changes, *Proceedings of the Royal Society of London A: Mathematical, Physical and Engineering Sciences*. **392**(1802), 45–57, (1984). ISSN 0080-4630. doi: 10.1098/rspa.1984.0023. URL <http://rspa.royalsocietypublishing.org/content/392/1802/45>.
26. M. J. Escuti, J. Kim, and M. W. Kudenov, Controlling light with geometric-phase holograms, *Opt. Photon. News*. **27**(2), 22–29 (Feb, 2016). doi: 10.1364/OPN.27.2.000022. URL <http://www.osa-opn.org/abstract.cfm?URI=opn-27-2-22>.
27. M. N. Miskiewicz and M. J. Escuti, Direct-writing of complex liquid crystal patterns, *Opt. Express*. **22**(10), 12691–12706 (May, 2014). doi: 10.1364/OE.22.012691. URL <http://www.opticsexpress.org/abstract.cfm?URI=oe-22-10-12691>.
28. R. K. Komanduri, K. F. Lawler, and M. J. Escuti, Multi-twist retarders: broadband retardation control using self-aligning reactive liquid crystal layers, *Opt. Express*. **21**(1), 404–420 (Jan, 2013). doi: 10.1364/OE.21.000404. URL <http://www>.

- [opticsexpress.org/abstract.cfm?URI=oe-21-1-404](http://www.opticsexpress.org/abstract.cfm?URI=oe-21-1-404).
29. G. P. P. L. Otten, F. Snik, M. A. Kenworthy, M. N. Miskiewicz, M. J. Escuti, and J. L. Codona. The vector apodizing phase plate coronagraph: prototyping, characterization and outlook. In *Society of Photo-Optical Instrumentation Engineers (SPIE) Conference Series*, vol. 9151, pp. 91511R–91511R–10, (2014). doi: 10.1117/12.2056096. URL <http://dx.doi.org/10.1117/12.2056096>.
  30. G. J. Ruane, E. Huby, O. Absil, D. Mawet, C. Delacroix, B. Carlomagno, and G. A. Swartzlander, Lyot-plane phase masks for improved high-contrast imaging with a vortex coronagraph, *A&A*. 583:A81 (Nov., 2015). doi: 10.1051/0004-6361/201526561.
  31. F. Snik, G. Otten, M. Kenworthy, D. Mawet, and M. Escuti. Combining vector-phase coronagraphy with dual-beam polarimetry. In *Ground-based and Airborne Instrumentation for Astronomy V*, vol. 9147, *Proc. SPIE*, p. 91477U (Aug., 2014). doi: 10.1117/12.2055452.
  32. M. J. Wilby, C. U. Keller, F. Snik, V. Korkiakoski, and A. G. M. Pietrow, The coronagraphic Modal Wavefront Sensor: a hybrid focal-plane sensor for the high-contrast imaging of circumstellar environments, *A&A* . 597:A112 (Jan., 2017). doi: 10.1051/0004-6361/201628628.